

# Dalton Transactions

Accepted Manuscript



This is an *Accepted Manuscript*, which has been through the Royal Society of Chemistry peer review process and has been accepted for publication.

*Accepted Manuscripts* are published online shortly after acceptance, before technical editing, formatting and proof reading. Using this free service, authors can make their results available to the community, in citable form, before we publish the edited article. We will replace this *Accepted Manuscript* with the edited and formatted *Advance Article* as soon as it is available.

You can find more information about *Accepted Manuscripts* in the [Information for Authors](#).

Please note that technical editing may introduce minor changes to the text and/or graphics, which may alter content. The journal's standard [Terms & Conditions](#) and the [Ethical guidelines](#) still apply. In no event shall the Royal Society of Chemistry be held responsible for any errors or omissions in this *Accepted Manuscript* or any consequences arising from the use of any information it contains.



Journal Name

ARTICLE

## A comparison of MOP-phosphonite ligands and their applications in Rh(I)- and Pd(II)-catalysed asymmetric transformations

James T. Fleming, Corinne Wills, Paul G. Waddell, Ross W. Harrington and Lee J. Higham\*

Received 00th January 20xx,  
Accepted 00th January 20xx

DOI: 10.1039/x0xx00000x

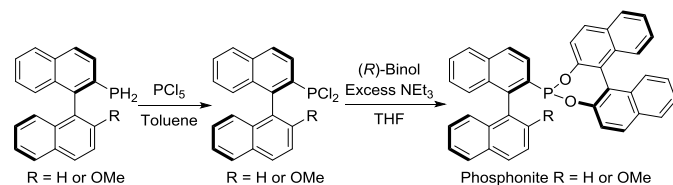
www.rsc.org/

Six chiral MOP-phosphonites have been synthesised and compared via experimental and computational methods in an effort to quantify their differing structural and electronic profiles. They were found to be electron-poor ligands in comparison to their arylphosphine analogues and have a larger *trans* influence in square planar Pt(II) complexes. Four [Rh(L<sup>P</sup>)(η<sup>2</sup>:η<sup>2</sup>-cod)Cl] complexes were synthesised and characterised by NMR, HRMS and X-ray crystallography. Two [Rh(L<sup>P</sup>)<sub>2</sub>]BF<sub>4</sub> complexes were prepared where one ligand acts as a chelating P,C-π-donor; detailed NMR studies demonstrated a hemilabile η<sup>6</sup>-coordination mode, which in one case was confirmed by X-ray crystallography. Rh(I) complexes were used as catalysts in asymmetric hydrogenation and hydroformylation reactions and in the addition of phenyl boronic acid to an isatin. Pd(II) complexes were successfully employed in asymmetric Suzuki-Miyaura cross-coupling reactions yielding binaphthyl products. Two [Pd(L<sup>P</sup>)<sub>2</sub>]Cl<sub>2</sub> complexes were synthesised and characterised by X-ray crystallography, both adopting *cis* orientations, with one of the complexes crystallising as two *pseudo*-polymorphs.

### Introduction

Organophosphorus compounds are a popular choice of ligand in homogeneous catalysis because their electronic and steric properties, and those of derived complexes, can be tuned.<sup>1</sup> Chiral monophosphorus ligands have found applications in a variety of organometallic catalysis, however they are often neglected in favour of the more established diphosphorus ligand class.<sup>2</sup> Therefore, we are keen to explore the potential of such ligands, especially those with unusual functionality on the phosphorus.<sup>3</sup> Phosphonites are valuable ligands used in homogeneous catalysis, with characteristic properties of being poor σ-donors but strong π-acceptors; the energy of their σ\* orbitals is lowered compared to those of related arylphosphines due to the electronegative substituents, allowing the ligand to better stabilise transition metals in low oxidation states. We reported a convenient synthetic route to enantiopure MOP-phosphonite ligands, which can act in a monodentate or hemilabile fashion, via air-stable, chiral primary phosphines (Scheme 1).<sup>4</sup>

**Scheme 1** Our synthesis of MOP-phosphonite ligands with two chiral centres.



School of Chemistry, Bedson Building, Newcastle University, Newcastle upon Tyne, NE1 7RU, UK. E-mail: lee.higham@ncl.ac.uk

Electronic Supplementary Information (ESI) available: Full experimental and crystallographic data. CCDC 1483130 (*R*)-**6b**, 1483131 (*S*)-**8a**, 1483132 (*R*)-**8b**, 1483133 (*S*)-**9a**, 1483134 (*R*)-**9b**, 1483871 (*R*)-**10b**, 1483135 (*S*)-**11a** (polymorph 1), 1483136 (*S*)-**11a** (polymorph 2) and 1483137 (*R*)-**11b**. For ESI and crystallographic data in CIF or other electronic format see DOI: 10.1039/x0xx00000x

Chiral phosphonite complexes are proven catalysts for a range of enantioselective reactions, including nickel-catalysed hydrocyanations,<sup>5</sup> palladium-catalysed hydrovinylations<sup>6</sup> and rhodium-catalysed hydroformylations<sup>7</sup> and hydrogenations.<sup>8</sup> Furthermore, our MOP-phosphonites in Scheme 1 were shown to be effective ligands in the palladium-catalysed asymmetric hydrosilylation of styrenes.<sup>4a</sup> In a follow-up communication we prepared the ligands in Chart 1, and showed that despite the presence of only one element of chirality compared to those ligands in Scheme 1, they were still highly effective in the palladium-catalysed hydrosilylation of substituted styrenes.<sup>4c</sup> In this work we investigate the ramifications of this structural modification on the stereoelectronic properties of the ligands, their coordination chemistry and the catalytic properties of the resultant transition metal complexes. Specifically the ligands (*S*)-**1a**, (*R*)-**1b**, (*S*)-**2a**, (*R*)-**2b**, (*S*)-**3a** and (*R*)-**3b** (Chart 1) were prepared, as well as their corresponding selenides, and our subsequent investigations allowed us to make quantitative comparisons of these donors, capturing their steric and electronic properties. We used DFT calculations to probe the frontier molecular orbitals of the ligands and we also present calculations which support our experimental observations that rotation about the C–C bond in the biphenyl moiety of (*S*)-**2a**, (*R*)-**2b**, (*S*)-**3a** and (*R*)-**3b** is unrestricted under typical conditions.<sup>4c</sup> The rhodium(I) and palladium(II) coordination chemistry of the ligands was then investigated in some detail by multinuclear NMR spectroscopy and X-ray crystallography. Finally the performance of the MOP-phosphonites as ligands in asymmetric hydrogenation, hydroformylation and Suzuki-Miyaura cross-coupling reactions was assessed and compared to that of the analogous phosphines MeO-MOP and H-MOP.

## Results and discussion

### Ligand Properties

#### Organophosphorus selenides

We synthesised  $R_3P(Se)$  by reacting the corresponding phosphorus ligand ( $L^P$ ) with an excess of potassium selenocyanate in THF at 50 °C. The  $^{31}P\{^1H\}$  NMR of the reaction product consists of a singlet with  $^{77}Se$  ( $I = \frac{1}{2}$ , natural abundance 7.6%) satellites (Table 1); the difference in chemical shift between  $L^P(Se)$  and  $L^P$  is *ca.* 50 ppm and downfield for the arylphosphines MeO-MOP and H-MOP, but larger (*ca.* 65–75 ppm) and upfield for the phosphonites. The magnitude of the  $^1J$  ( $^{31}P-^{77}Se$ ) coupling can provide an indication of the  $\sigma$ -donor strength of the parent phosphorus lone pair, which is inversely correlated to the coupling constant.<sup>9</sup> The data implies that our MOP-phosphonites (906–930 Hz) are relatively weak  $\sigma$ -donors compared to their electron-rich aryl analogues (720–723 Hz) due to the increased electron-withdrawing effects of the oxygen-containing substituents, which results in the phosphorus lone pair having a larger s- and lower p-character, and a decreased  $\sigma$ -basicity (Table 1). The  $^1J_{PSe}$  values for the MOP-phosphonites **1-3** are also larger than those we recently reported for analogous MOP phosphonites with two methoxy substituents bound to the phosphorus (858 and 860 Hz),<sup>3</sup> indicating that replacing two alkoxy functionalities with aryloxy groups results in ligands that are weaker  $\sigma$ -donors in this selenide series.

It has been demonstrated that the presence of bulky substituents on the phosphorus atom can result in a lower value for the coupling constant (i.e. a decrease in the s-character of the lone pair),<sup>10</sup> which may explain why the bulky dimethylbiphenoxy phosphonites (*S*)-**3a** and (*R*)-**3b** have lower  $^1J_{PSe}$  values than the biphenoxy phosphonites (*S*)-**2a** and (*R*)-**2b**.

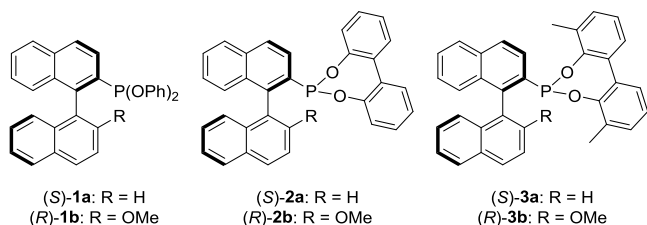


Chart 1 Phosphonite ligands (*S*)-**1a**, (*R*)-**1b**, (*S*)-**2a**, (*R*)-**2b**, (*S*)-**3a** and (*R*)-**3b**.

**Table 1** Selected  $^{31}P\{^1H\}$  NMR spectroscopic data for  $L^P(Se)$  compounds and IR spectroscopic data for  $trans-[Rh(L^P)_2(CO)Cl]$  complexes.

Ligand	$\delta$ ( $L^P(Se)$ ) <sup>c</sup>	$^1J_{PSe}$ ( $L^P(Se)$ ) <sup>d</sup>	$\Delta\delta$ <sup>e</sup>	$\nu(CO)$ <sup>e,f</sup>
( <i>S</i> )-H-MOP <sup>a</sup>	36.6	723	+ 50.2	1968
( <i>R</i> )-MeO-MOP <sup>b</sup>	38.3	720	+ 52.0	1974
( <i>S</i> )- <b>1a</b> <sup>a</sup>	89.4	908	– 65.4	2006
( <i>R</i> )- <b>1b</b> <sup>a</sup>	91.7	906	– 63.9	2002
( <i>S</i> )- <b>2a</b> <sup>a</sup>	104.1	926	– 74.5	2005
( <i>R</i> )- <b>2b</b> <sup>a</sup>	104.4	930	– 75.6	1997
( <i>S</i> )- <b>3a</b> <sup>a</sup>	105.4	918	– 67.0	2006
( <i>R</i> )- <b>3b</b> <sup>a</sup>	103.9	915	– 70.3	2005

<sup>a</sup> NMR measurements were taken at 162 MHz in  $CDCl_3$ . <sup>b</sup> NMR measurements were taken at 202 MHz in  $CDCl_3$ . <sup>c</sup> Chemical shift in ppm. <sup>d</sup> Coupling constant in Hz. <sup>e</sup>  $\Delta\delta = \delta(L^P(Se)) - \delta(L^P)$  in ppm. <sup>f</sup> IR measurements were taken as solutions in DCM. <sup>f</sup> Symmetric carbonyl stretching frequency in  $cm^{-1}$ .

### Rhodium(I) Vaska-type complexes

Another important indicator of the net-donor properties of  $PR_3$  ligands is the symmetric carbonyl stretching frequency ( $\nu(CO)$ ) in the IR spectrum of  $trans-[Rh(L^P)_2(CO)Cl]$  complexes (Table 1).<sup>11</sup> The complexes are prepared by reaction of four equivalents of the phosphorus ligand with  $[Rh(CO)_2Cl]_2$ ,<sup>12</sup> and do not exhibit the high toxicity associated with the nickel(0) carbonyl complexes traditionally used, although the data does correlate well with the Tolman values.<sup>11,13</sup> A low value for  $\nu(CO)$  indicates that the ligand is a strong electron donor, conversely, a high value for  $\nu(CO)$  indicates low net donor properties. The values for our phosphonites (1997–2006  $cm^{-1}$ ) indicate overall low net-donor properties compared to the MOP-phosphine ligands (1968–1974  $cm^{-1}$ ) (Table 1), as would be expected for this ligand class which are poor  $\sigma$ -donors but strong  $\pi$ -acceptors; the reduced electron density on the rhodium atom results in less  $\pi$ -back-bonding with the carbonyl group, resulting in a stronger CO bond and hence an increase in  $\nu(CO)$ .<sup>11b</sup>

### Platinum(II) complexes

(*S*)-H-MOP, (*R*)-MeO-MOP and each phosphonite was reacted with the platinum precursor  $[Pt(PET_3)_2Cl_2]$  in  $CD_2Cl_2$  to generate the unsymmetrical platinum(II) complexes  $trans-[Pt((S)\text{-H-MOP})(PET_3)_2Cl_2]$  (*S*)-**4a**,  $trans-[Pt((R)\text{-MeO-MOP})(PET_3)_2Cl_2]$  (*R*)-**4b**,  $trans-[Pt((S)\text{-1a})(PET_3)_2Cl_2]$  (*S*)-**5a**,  $trans-[Pt((R)\text{-1b})(PET_3)_2Cl_2]$  (*R*)-**5b**,  $trans-[Pt((S)\text{-2a})(PET_3)_2Cl_2]$  (*S*)-**6a**,  $trans-[Pt((R)\text{-2b})(PET_3)_2Cl_2]$  (*R*)-**6b**,  $trans-[Pt((S)\text{-3a})(PET_3)_2Cl_2]$  (*S*)-**7a** and  $trans-[Pt((R)\text{-3b})(PET_3)_2Cl_2]$  (*R*)-**7b** via bridge cleavage reactions.<sup>14</sup> We observed exclusively the formation of the *trans* isomers in the  $^{31}P\{^1H\}$  NMR spectra of the compounds (Table 2).<sup>15</sup> The value of  $\delta$  ( $L^P$ ) for the complexes with the phosphonite ligands was shifted *ca.* 30–50 ppm upfield compared to the resonance of the free ligand, the phenoxy derived ligands having the largest shift and the *ortho*-methyl substituted biphenoxy ligands the lowest; the phosphine ligands were shifted *ca.* 35–40 ppm downfield (Table 2). The values of the  $^2J_{PP}$  coupling between the ligands are relatively high and characteristic of a *trans* geometry.<sup>16</sup> The phosphonite complexes show little variance (*ca.* 620 Hz) and the values are noticeably larger than those for the phosphine ligands (*ca.* 470 Hz).

We sought to determine the relative *trans* influence of our series of MOP-ligands by measuring the  $^1J$  ( $^{31}P-^{195}Pt$ ) coupling for  $Pt-PEt_3$  in the square-planar platinum(II) complexes ( $^{195}Pt$ ,  $I = \frac{1}{2}$ , natural abundance 33.8%) (Table 2).<sup>14,17</sup> We found that the *trans* influence of our phosphonites (2382–2519 Hz, Table 2, entries 3–8) is larger than that found for the aryl analogues (2554–2574 Hz, Table 2, entries 1 and 2); a smaller  $^1J_{PPt}$  coupling to  $PEt_3$  denotes a larger *trans* influence from  $L^P$ . The coupling constant for the *ortho*-methyl substituted biphenoxy phosphonites (Table 2, entries 7 and 8) was noticeably lower than that for the phenoxy and biphenoxy phosphonites (Table 2, entries 3–6) which were all within a range of 29 Hz, implying that ligands (*S*)-**3a** and (*R*)-**3b** have the largest *trans* influence in the series.

We were able to obtain single crystals suitable for X-ray crystallography for one of our platinum(II) complexes, (*R*)-**6b** (Fig. 1), by slow diffusion of diethyl ether into a  $CD_2Cl_2$  solution.

There is a *pseudo* square-planar geometry around the platinum atom; both (*R*)-**6b** and  $\text{PEt}_3$  show monodentate coordination through the phosphorus atom and are *trans* to each other with a P–Pt–P bond angle of  $170.36(4)^\circ$ . The Pt– $\text{PEt}_3$  bond length ( $2.3148(11)$  Å) is similar to that reported for an analogous phosphonite complex, containing a fluorine-substituted derivative of diphenyl phenylphosphonite, which has two independent molecules in the unit cell ( $2.321(4)$  and  $2.319(4)$  Å).<sup>18</sup> The Pt– $\text{PEt}_3$  bond length in (*R*)-**6b** is longer than that in the related MOP-bis(dimethylamino)phosphine and MOP-phosphirane complexes that we recently reported as part of our study into the stereoelectronic profiles of a series of MOP-type ligands, which have analogous bond lengths of  $2.3050(15)$  Å and  $2.284(3)$  Å respectively, indicating that the phosphonite ligand has the largest *trans* influence of the three.<sup>3</sup>

It is cautionary to note however, that the  $^1J_{\text{Pt}}$  coupling for  $\text{PEt}_3$  in (*R*)-**6b** ( $2503$  Hz, Table 2, Entry 6) is significantly larger than reported for the MOP-bis(dimethylamino)phosphine complex ( $2365$  Hz),<sup>3</sup> which as discussed would imply that the phosphonite ligand exhibits a weaker *trans* influence - this contradiction may be due to steric effects in the solid state. We are not aware of any analogous bis(dimethylamino)phosphine complexes for comparison.

**Table 2** Selected  $^{31}\text{P}\{^1\text{H}\}$  NMR spectroscopic data for *trans*-[Pt( $L^P$ )( $\text{PEt}_3$ ) $\text{Cl}_2$ ] complexes.

Complex	$\delta$ ( $L^P$ ) <sup>c</sup>	$^1J_{\text{Pt}}(L^P)$ <sup>d</sup>	$\delta$ ( $\text{PEt}_3$ ) <sup>c</sup>	$^1J_{\text{Pt}}(\text{PEt}_3)$ <sup>d</sup>	$^2J_{\text{PP}}$ <sup>d</sup>
1 ( <i>S</i> )- <b>4a</b> <sup>a</sup>	21.5	2437	13.8	2574	473
2 ( <i>R</i> )- <b>4b</b> <sup>b</sup>	25.3	2440	13.7	2554	468
3 ( <i>S</i> )- <b>5a</b> <sup>a</sup>	111.8	3481	11.2	2495	621
4 ( <i>R</i> )- <b>5b</b> <sup>a</sup>	108.8	3467	9.0	2519	618
5 ( <i>S</i> )- <b>6a</b> <sup>a</sup>	140.6	3520	10.0	2490	624
6 ( <i>R</i> )- <b>6b</b> <sup>a</sup>	140.5	3517	9.0	2503	620
7 ( <i>S</i> )- <b>7a</b> <sup>a</sup>	140.5	3521	8.6	2398	620
8 ( <i>R</i> )- <b>7b</b> <sup>a</sup>	142.6	3541	12.1	2382	620

<sup>a</sup> NMR measurements were taken at 162 MHz in  $\text{CD}_2\text{Cl}_2$ . <sup>b</sup> NMR measurements were taken at 202 MHz in  $\text{CD}_2\text{Cl}_2$ . <sup>c</sup> Chemical shift in ppm. <sup>d</sup> Coupling constant in Hz.

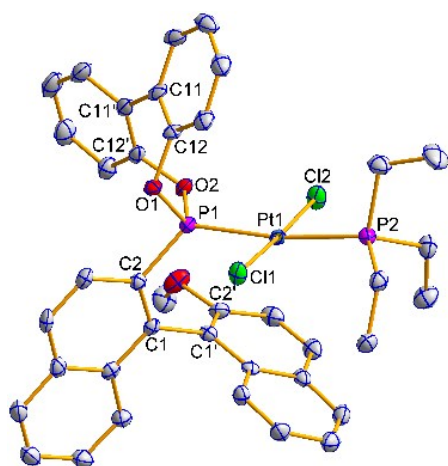


**Fig. 1** Molecular structure of (*R*)-**6b**. Hydrogen atoms have been omitted for clarity. Selected average bond distances (Å) and angles ( $^\circ$ ): Pt1–P1  $2.2703(10)$ , Pt1–P2  $2.3148(11)$ , Pt1–Cl1  $2.3203(10)$ , Pt1–Cl2  $2.2873(10)$ , P1–C2  $1.813(4)$ , P1–O1  $1.612(3)$ , P1–O2  $1.607(3)$ , P1–Pt1–Cl1  $85.72(4)$ , P1–Pt1–P2  $170.36(4)$ , P1–Pt1–Cl2  $94.02(4)$ , C2–C1–C1'–C2'  $-87.6(5)$ , C12–C11–C11'–C12'  $-43.2(6)$ .

## DFT calculations

We have performed Density Functional Theory (DFT) calculations on the optimised structures of the MOP-ligands using the B3LYP functional with a 6-31G\* basis set to calculate the frontier molecular orbital energies (Table 3), the Highest Occupied Molecular Orbital ( $E_{\text{HOMO}}$ ) and Lowest Unoccupied Molecular Orbital ( $E_{\text{LUMO}}$ ).<sup>19</sup>  $E_{\text{HOMO}}$  typically contains the phosphorus lone pair in tertiary phosphines and can be used as an indication of the ligand  $\sigma$ -donor strength.<sup>20</sup> The values for  $E_{\text{HOMO}}$  are invariably lower for the H-MOP molecules compared to their MeO-MOP analogues (Table 3), implying that the latter have stronger  $\sigma$ -donor properties, in agreement with calculations for related ligands previously reported.<sup>3</sup> The HOMO energies for the H-MOP phosphonites are lower than that for their arylphosphine counterpart, and this trend also holds true for the MeO-MOP ligand family, implying the phosphonites are weaker P-ligand  $\sigma$ -donors in each series. However, note that the MeO-MOP phosphonite (*R*)-**3b** has a *higher* calculated HOMO energy ( $-5.48$  eV) than the phosphine H-MOP ( $-5.48$  eV).  $E_{\text{LUMO}}$  may be invoked in back-bonding,<sup>19</sup> and the lower values for these phosphonites compared to the phosphines suggests they will likely have better  $\pi$ -acceptor properties (Table 3); the H-MOP phosphonites have lower LUMO energies than their 2'-methoxy-substituted analogues. One of the earliest methods developed for quantifying the steric effects of phosphorus ligands is the Tolman cone angle ( $\theta$ );<sup>13</sup> however, for MOP-type ligands where the substituent groups differ greatly, the values obtained may not best reflect the properties of the ligand.<sup>21</sup> An alternative means of evaluating the steric bulk of phosphorus ligands is the symmetric deformation coordinate ( $S4'$ ), introduced by Orpen and co-workers using data obtained from crystal structures.<sup>22</sup>  $S4'$  seeks to evaluate the ligands based on a geometric calculation using phosphine angles from species with the general formula  $Z\text{-PR}_3$  ( $Z$  = transition-, main group- or non-metal). It has also been shown that  $S4'$  values can be calculated with sufficient accuracy to the data obtained from X-ray crystallographic analysis of phosphine complexes.<sup>23</sup> We therefore used the DFT optimised structures for the series of MOP-ligands in Table 3 to calculate a modified descriptor of  $S4'$  ( $S4$ ), calculating  $Z$  to be a vector perpendicular to the plane containing the three substituents on the phosphorus.<sup>24</sup>

**Table 3** Calculated HOMO and LUMO energies and symmetric deformation coordinate values for the MOP-ligands discussed in this study.

Ligand	$E_{\text{LUMO}}^{\text{a,b}}$	$E_{\text{HOMO}}^{\text{a,b}}$	$S4^{\text{a,c}}$	$S4^{\text{c,d}}$
( <i>S</i> )-H-MOP	-1.15	-5.51	41	–
( <i>R</i> )-MeO-MOP	-1.06	-5.27	42	–
( <i>S</i> )- <b>1a</b>	-1.29	-5.80	54	–
( <i>R</i> )- <b>1b</b>	-1.21	-5.51	54	66/70 <sup>e</sup>
( <i>S</i> )- <b>2a</b>	-1.33	-5.76	58	–
( <i>R</i> )- <b>2b</b>	-1.21	-5.47	58	60
( <i>S</i> )- <b>3a</b>	-1.34	-5.76	58	–
( <i>R</i> )- <b>3b</b>	-1.22	-5.48	58	–

<sup>a</sup> Calculated at the DFT level of theory using the B3LYP functional with a 6-31G\* basis set.

<sup>b</sup> Energies in eV. <sup>c</sup> Symmetric deformation coordinate in degrees. <sup>d</sup> Calculated from X-ray data. <sup>e</sup> The asymmetric unit comprises two molecules in different conformations.



For phosphines, small values for  $S_4$  can suggest substituents with increasing steric bulk. Our values for (*S*)-H-MOP and (*R*)-MeO-MOP (Table 3) are close to those calculated for PPh<sub>3</sub> (39.6°) by Suresh and co-workers,<sup>24</sup> implying that they have a similar steric profile. The  $S_4$  values for the MOP-phosphonite ligands are approximately 12–17° larger than their phosphine analogues, and show little variation between themselves. However, it is more difficult to accurately model compounds with P–O bonds compared to P–C bonds, since the R groups in P(OR)<sub>3</sub> compounds are much further from the phosphorus than in PR<sub>3</sub> ligands. Therefore the accuracy of this method may not be suitable to our MOP-phosphonite ligands due to their conformational flexibility.<sup>23</sup>

We recently reported the solid state structures of (*R*)-**1b** and (*R*)-**2b**,<sup>4c</sup> and consequently here we have been able to calculate  $S_4$  from the X-ray crystallographic data and compare it to the computed structures (Table 3). The  $S_4$  value for (*R*)-**1b** is considerably larger in the X-ray structure compared to the calculated one, whereas both are similar for (*R*)-**2b**; the smaller  $S_4$  value for (*R*)-**2b** compared to (*R*)-**1b** is more consistent with what might be expected due to the biphenoxy group having less conformational flexibility. We then calculated the approximate barrier to rotation for the ligands (*S*)-**3a** and (*R*)-**3b**. Substituted biphenyls show conformational enantiomorphism, the ease with which isomerisation occurs depending on the size of the ortho substituents.<sup>25</sup> The peaks in the energy profile for rotation in biphenyl compounds generally occur at 0°, ±90° and 180°, when the two phenyl rings are either coplanar or orthogonal; the local minima occur near 45° either side of the secondary maxima at ±90 due to a compromise between the steric demands of the ortho-substituents and π-electron overlap.<sup>26</sup> The rotational barrier in 1,1'-biphenyl, and non-ortho-substituted biphenyls, are comparable at 0° and 90° (1.4–2.0 kcal/mol).<sup>26</sup> An activation energy barrier of approximately 23 kcal/mol is required to prevent spontaneous room temperature torsional-isomerisation of biphenyl derivatives.<sup>25d</sup> It is important to note that when calculating barriers to rotation the method and basis set employed have a large impact on the optimised torsion angles.<sup>25c,d</sup>

In our study, the torsion angle between the planes of the two phenyl rings (C12–C11–C11'–C12') was constrained at selected values and the optimised geometry calculated. We also calculated the idealised angle for the unconstrained molecule at each local minima; a plot of the relative energies versus the dihedral angle is shown in Fig. 2 (the values are provided in tabular format in ESI Table 3). The curves in the graph are not mirror images of each other, as the two minima are diastereomers and hence of unequal energy. The most stable torsional angles for (*S*)-**3a** and (*R*)-**3b** were calculated to be –46.11° and –46.00° respectively (ESI Table 3). The calculated energy profiles for both (*S*)-**3a** and (*R*)-**3b** are very similar with an energy barrier of approximately 7–8 kcal/mol when the biphenyl rings are coplanar, a value far below the 23 kcal/mol barrier reported as being required to prevent spontaneous racemisation at room temperature.<sup>25d</sup> This result concurs with our experimental findings that rotation about the aryl–aryl junction is unrestricted under standard conditions (*vide infra*).

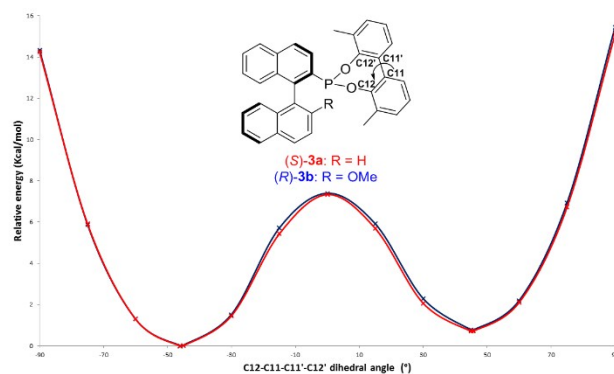


**Fig. 2** Calculated conformational energy differences (in kcal/mol) versus dihedral angle for the ligands (*S*)-**3a** and (*R*)-**3b** (in °), relative to the energy at the optimised dihedral angle; (*S*)-**3a** (red) and (*R*)-**3b** (blue). The geometry optimisations were performed at the DFT level of theory using the B3LYP functional with a 6-31G\* basis set.

### Rhodium(I) complexes and catalysis

Successful examples of rhodium-catalysed asymmetric transformations employing MOP-type ligands can be found in the literature. Recently Shintani, Nozaki and co-workers reported the high yielding and enantioselective synthesis of silicon-stereogenic dibenzosiloles<sup>27</sup> and the intramolecular alkynylsilylation of alkynes.<sup>28</sup> MeO-MOP and P-stereogenic phosphine derivatives have shown promise in the rhodium-catalysed asymmetric addition of phenyl boronic acid to naphthaldehyde.<sup>29</sup> Asymmetric intramolecular hydroamination of unactivated alkenes using a rhodium(I) catalyst has been described by Shen and Buchwald, who used a series of binaphthyl-based monophosphine ligands to give high yields and up to 91% *ee* with the substrates tested.<sup>30</sup>

### [Rh(L<sup>P</sup>)(η<sup>2</sup>:η<sup>2</sup>-cod)Cl] complexes

Phosphonites (*S*)-**2a**, (*R*)-**2b**, (*S*)-**3a** and (*R*)-**3b** were reacted with [Rh(η<sup>2</sup>:η<sup>2</sup>-cod)Cl]<sub>2</sub> in a 1:1, P:Rh ratio, to quantitatively give the chloro(1,5-cyclooctadiene)rhodium(I) complexes [Rh((*S*)-**2a**)(η<sup>2</sup>:η<sup>2</sup>-cod)Cl] (*S*)-**8a**, [Rh((*R*)-**2b**)(η<sup>2</sup>:η<sup>2</sup>-cod)Cl] (*R*)-**8b**, [Rh((*S*)-**3a**)(η<sup>2</sup>:η<sup>2</sup>-cod)Cl] (*S*)-**9a** and [Rh((*R*)-**3b**)(η<sup>2</sup>:η<sup>2</sup>-cod)Cl] (*R*)-**9b**. The analogous reactions with (*S*)-**1a** and (*R*)-**1b** were also attempted, however the resultant complexes were very sensitive to decomposition and we were unable to isolate them. Three of the four rhodium complexes gave broadened <sup>31</sup>P{<sup>1</sup>H} NMR spectral signals at room temperature, therefore they were analysed by variable temperature (VT) NMR spectroscopy (see ESI). For (*S*)-**8a** we observed a broad doublet at 25 °C which became clearer upon heating to 50 °C (δ = 162.9 ppm and <sup>1</sup>J<sub>PRh</sub> = 224 Hz); cooling the sample down to –55 °C resulted in the observation of two distinct species with relative intensities of ~65% (δ = 164.6 ppm and <sup>1</sup>J<sub>PRh</sub> = 223 Hz) and ~35% (δ = 161.4 ppm and <sup>1</sup>J<sub>PRh</sub> = 221 Hz). For (*R*)-**8b** a doublet was observed at 25 °C (δ = 163.3 ppm and <sup>1</sup>J<sub>PRh</sub> = 221 Hz), and cooling down to –55 °C resulted in the appearance of an additional upfield low intensity doublet resonance. The two species which appear in the spectra of (*S*)-**8a** and (*R*)-**8b** at –55 °C most likely correspond to conformational isomers with the ligands exhibiting restricted rotation about the biphenyl C–C bridge. Both (*S*)-**8a** and (*R*)-**8b** were poorly soluble in CDCl<sub>3</sub> and CD<sub>2</sub>Cl<sub>2</sub>, which proved to be problematic when performing NMR experiments due to the

high number of scans required; presumably at low temperatures the complexes precipitate out of the solution reducing the concentration further. However, we were able to characterise the binaphthyl moiety in (*S*)-**8a** at 50 °C and (*R*)-**8b** at 25 °C, but the broadened  $^1\text{H}$  and  $^{13}\text{C}$  resonances attributed to the biphenyl moieties could not be assigned.

For the dimethylbiphenoxy phosphonite complex (*S*)-**9a**, phosphonite coordination resulted in one broad  $^{31}\text{P}\{^1\text{H}\}$  NMR signal at 25 °C which split into a poorly resolved doublet when heated to 50 °C. Cooling to -55 °C allowed for the resolution of three signals with approximate ratios of 76% ( $\delta = 170.2$  ppm,  $^1J_{\text{PRh}} = 225$  Hz), 14% ( $\delta = 169.4$  ppm,  $^1J_{\text{PRh}} = 224$  Hz) and 10% ( $\delta = 162.0$  ppm,  $^1J_{\text{PRh}} = 223$  Hz). The methoxy analogue (*R*)-**9b** shows a broad doublet coupling at 25 °C, whose resolution improved upon heating to 50 °C; cooling to -55 °C resulted in the formation of five distinct doublets with approximate ratios of 13% ( $\delta = 168.1$  ppm,  $^1J_{\text{PRh}} = 227$  Hz), 80% ( $\delta = 167.5$  ppm,  $^1J_{\text{PRh}} = 226$  Hz), 1% ( $\delta = 165.1$  ppm,  $^1J_{\text{PRh}} = 227$  Hz), 3% ( $\delta = 163.4$  ppm,  $^1J_{\text{PRh}} = 224$  Hz) and 3% ( $\delta = 162.8$  ppm,  $^1J_{\text{PRh}} = 223$  Hz). The multiple species observed in the  $^{31}\text{P}\{^1\text{H}\}$  NMR of (*S*)-**9a** and (*R*)-**9b** at -55 °C most likely correspond to rotamers.

2D phase-sensitive  $^{31}\text{P}\{^1\text{H}\}$  EXSY NMR experiments have been used to study the mechanism for dynamic ligand exchange in chiral rhodium<sup>31</sup> phosphine complexes, as well as quantitative kinetic analysis of terminal ligand redistribution in a nickel phosphine complex.<sup>32</sup> An EXSY NMR experiment was recorded to detect any dynamic ligand exchange in (*S*)-**9a** and (*R*)-**9b**; measurements were taken at -55 °C with a mixing time of 100 ms (see ESI). The absence of cross-peaks in the spectra indicates that the three distinct chemical species observed in (*S*)-**9a** and the five distinct chemical species observed in (*R*)-**9b** do not participate in dynamic exchange at this temperature.

X-ray crystal structures were determined for (*S*)-**8a**, (*R*)-**8b**, (*S*)-**9a** and (*R*)-**9b** (Fig. 3 and ESI Figs. 2-6). In the asymmetric unit of both (*S*)-**9a** and (*R*)-**9b** there are two molecules in different conformations - an overlay of the crystallographically independent molecules in (*R*)-**9b** is provided to highlight that the torsion angle of the dimethyl substituted biphenyl moiety is of opposite sign in the two molecules (ESI Fig. 10). There is a *pseudo*-square-planar geometry around the rhodium and the Rh-P bond lengths range from 2.2104(13) Å in (*R*)-**8b** to 2.2428(13) Å in (*R*)-**9b**, consistent with the literature value of 2.2112(7) Å for an analogous MeO-MOP-phosphonite complex which we ourselves reported<sup>4b</sup> and 2.233(2) Å for a related complex employing a hydroxy phosphonite ligand.<sup>33</sup> The Rh-Cl bond lengths are longer than the Rh-P bond lengths and range from 2.3470(13) Å in (*R*)-**9b** (Fig. 3) to 2.3757(12) Å in (*R*)-**8b** (see ESI Fig. 3); the corresponding literature values (*vide supra*) of 2.3661(8) Å<sup>4b</sup> and 2.371(2) Å<sup>33</sup> lie within this range. The phosphorus donor shows a stronger *trans* influence compared to the chloride in each case, hence for the alkene *trans* to the phosphorus, the C-C bond is shorter and the Rh-C bonds are longer than the alkene bound *cis* to the phosphorus atom. In (*S*)-**8a** and (*R*)-**8b** the lower naphthyl fragment of the binaphthyl backbone is face-to-face with the rhodium centre, whereas in both independents of (*S*)-**9a** and (*R*)-**9b** it is orientated away from the rhodium centre and faces the biphenyl moiety.

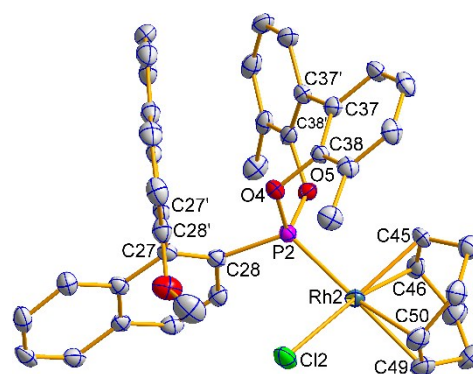


**Fig. 3** Molecular structure of one of the two independent molecules of (*R*)-**9b** (the asymmetric unit comprises two molecules in different conformations). Hydrogen atoms have been omitted for clarity. Selected average bond distances (Å) and angles (°): Rh2-P2 2.2428(13), Rh2-Cl2 2.3470(13), Rh2-C45 2.131(5), Rh2-C46 2.134(5), Rh2-C49 2.272(6), Rh2-C50 2.237(5), P2-C28 1.823(5), P2-O4 1.609(3), P2-O5 1.615(4), C45-C46 1.399(8), C49-C50 1.330(8); P2-Rh2-Cl2 89.62(5), P2-Rh2-C49 173.59(16), P2-Rh2-C50 152.03(16), P2-Rh2-C45 92.60(15), P2-Rh2-C46 95.98(15), C28-C27'-C28' -104.6(6), C38-C37'-C38' -43.3(8).

### [Rh(L<sup>P</sup>)<sub>2</sub>]BF<sub>4</sub> complexes

We next synthesised [Rh(L<sup>P</sup>)<sub>2</sub>]<sup>+</sup> complexes using our bulky dimethylbiphenoxy ligands (*S*)-**3a** and (*R*)-**3b** by reacting two equivalents of the phosphonite with [Rh(η<sup>2</sup>:η<sup>2</sup>-cod)<sub>2</sub>]BF<sub>4</sub> to afford [Rh((*S*)-**3a**)<sub>2</sub>]BF<sub>4</sub> (*S*)-**10a** and [Rh((*R*)-**3b**)<sub>2</sub>]BF<sub>4</sub> (*R*)-**10b**. (*S*)-**10a** and (*R*)-**10b** were characterised by multinuclear NMR spectroscopy, HRMS and for (*R*)-**10b**, X-ray crystallography. Solution state  $^{31}\text{P}\{^1\text{H}\}$  VT NMR studies on (*S*)-**10a** and (*R*)-**10b** (see ESI) revealed that the two phosphorus nuclei are inequivalent, due to the appearance of two resonances with equal intensity, which are shifted slightly upfield compared to (*S*)-**9a** and (*R*)-**9b**. Upon cooling we were able to measure P-P and P-Rh coupling, which gave a doublet of doublets splitting pattern for (*S*)-**10a** ( $^1J_{\text{PRh}} = 288$  and 294 Hz and  $^2J_{\text{PP}} = 27$  Hz) and (*R*)-**10b** ( $^1J_{\text{PRh}} = 283$  and 310 Hz and  $^2J_{\text{PP}} = 32$  Hz).

The  $^1\text{H}$  resonances in the spectra of (*S*)-**10a** and (*R*)-**10b** were slightly broadened and unresolved at room temperature, however upon cooling to 5 °C and -20 °C respectively, we were able to observe the expected number of independent aromatic resonances (38 for (*S*)-**10a** and 36 for (*R*)-**10b**) and the 4 independent methyl resonances from the biphenoxy moieties. Using two dimensional NMR experiments ( $^1\text{H}$ -COSY,  $^1\text{H}$ -ROESY, HSQC and HMBC) performed at these reduced temperatures, in addition to  $^1\text{H}$ ,  $^1\text{H}\{^{31}\text{P}\}$  and  $^{13}\text{C}\{^1\text{H}\}$  NMR data, we were able to unambiguously assign the proton and carbon resonances. The  $^{13}\text{C}$  NMR chemical shift data for (*S*)-**10a** and (*R*)-**10b** reveal that in the solution state, one of the hemilabile MOP ligands is coordinating to the rhodium atom via an η<sup>6</sup>-binding mode using the lower naphthyl ring, in addition to bonding through the phosphorus atom (Fig. 4). The carbon atoms in the η<sup>6</sup>-bound C<sub>6</sub> ring from the P,C-π-donor ligand (B) are shifted upfield compared to those in the solely P-donor ligand (A), by a magnitude of 8.9 to 26.5 ppm in (*S*)-**10a** and 6.5 to 35.7 in (*R*)-**10b** (Fig. 4). The resonances attributed to C1' and C4' in ligand B are the most significantly shifted and appear as doublets with *J* values of 11.3 and 12.8 Hz in (*S*)-**10a** and 15.2 and 10.4 Hz in (*R*)-**10b** respectively (see ESI).

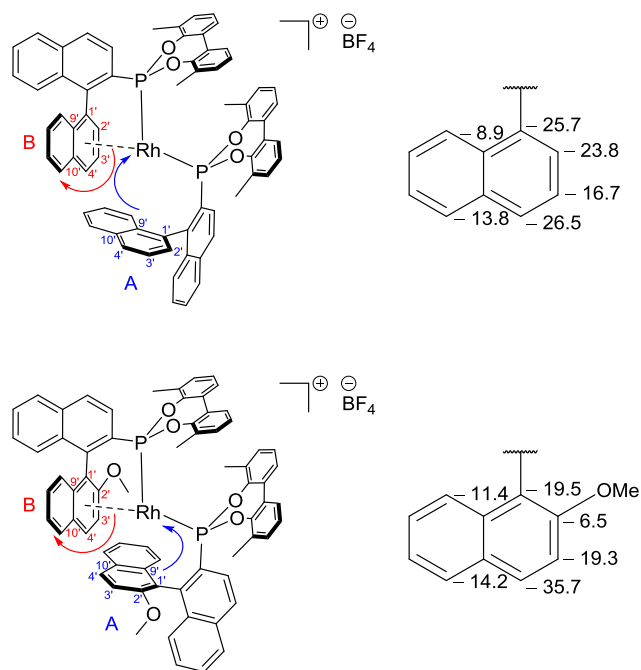


**Fig. 4** Proposed molecular structure and a fragment showing the <sup>13</sup>C{<sup>1</sup>H} NMR coordination chemical shift (ppm) of ligand B (P,C-π-donor) relative to that of ligand A (P-donor) for (S)-10a (top) and (R)-10b (bottom). NMR measurements were taken at 176 MHz in CDCl<sub>3</sub> at 5 °C for (S)-10a and at 126 MHz in CDCl<sub>3</sub> at -20 °C for (R)-10b.

The result of having a chelating P,C-π-donor is saturation of the rhodium coordination sphere. This may explain the increased stability of the [Rh(L<sup>P</sup>)<sub>2</sub>]BF<sub>4</sub> species compared to the 16 electron [Rh(L<sup>P</sup>)(η<sup>4</sup>-cod)Cl] complexes, which are prone to oxidation. The presence of dynamic behaviour in (S)-10a was probed by Rotating frame Overhauser Effect Spectroscopy (ROESY); the 2D phase-sensitive <sup>1</sup>H-ROESY NMR spectra in CDCl<sub>3</sub> at 0 °C and -50 °C are shown in Fig. 5. At 0 °C exchange is evident, a result of hemilabile binding of the η<sup>6</sup>-coordinated aryl which dissociates and is then replaced by the equivalent face of the second ligand (Fig. 4). Upon cooling to -50 °C this dynamic behaviour ceases. The X-ray crystal structure of (R)-10b shows there are two crystallographically independent molecules in the asymmetric unit, which comprises two cations and two BF<sub>4</sub> anions (Fig. 6 and ESI Fig. 7). The cations of (R)-10b contain a rhodium atom with two coordinated phosphonites; both ligands coordinate via the phosphorus atom and, in each case, one ligand acts as a chelating P,C-π-donor via a second binding mode using the lower naphthyl ring (Fig. 6 and ESI Fig. 7). The Rh-C distances suggest an η<sup>6</sup>-binding mode, consistent with our solution state NMR experiments, where we propose that the C<sub>6</sub> ring containing the *ipso*-C (which happens to be the closest contact) coordinates to the rhodium atom side-on via its π-system (*vide supra*). This η<sup>6</sup>-bonding motif for a MOP-type ligand is rare, the other example we are aware of is a MOP-phosphonite complex that we previously reported, with a BINOL moiety on the phosphorus atom - the Rh-C<sub>aryl</sub> distances in both complexes are comparable.<sup>4b</sup> Goldberg reported η<sup>6</sup>-bonding modes in rhodium complexes with 2-(dicyclohexylphosphino)biphenyl ligands.<sup>34</sup>

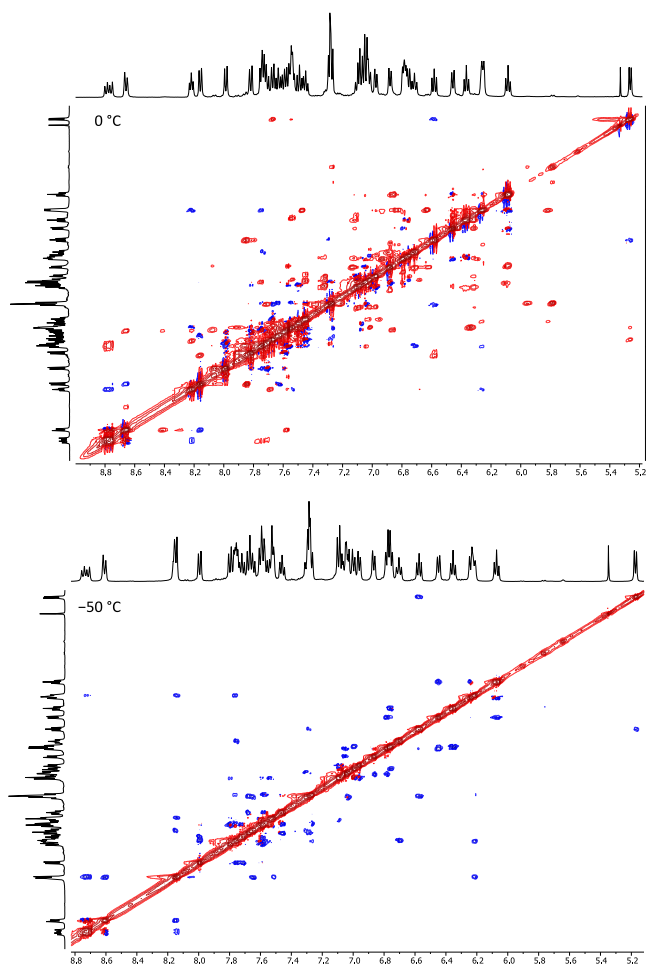


**Fig. 5** 2D phase-sensitive <sup>1</sup>H-ROESY NMR spectra of (S)-10a in CDCl<sub>3</sub> at 0 °C (top) and -50 °C (bottom), with a mixing time of 200 ms. The diagonal and exchange cross-peaks are phased positive (red) and the ROE signals are negative (blue).

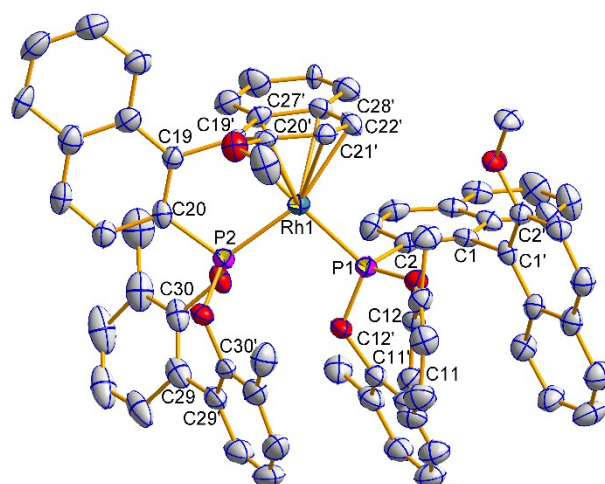


**Fig. 6** Molecular structure of one of the cations of (R)-10b (the asymmetric unit comprises two cations and two anions in different conformations). Hydrogen atoms have been omitted for clarity. Selected average bond distances (Å) and angles (°): Rh1-P1 2.2117(16), Rh1-P2 2.2008(18), Rh1-C19' 2.200(6), Rh1-C20' 2.311(6), Rh1-C21' 2.312(6), Rh1-C22' 2.278(7), Rh1-C27' 2.445(7), Rh1-C28' 2.492(6), P1-C2 1.816(6), P2-C20 1.817(7); P1-Rh1-P2 98.62(6), Rh1-P1-C2 111.1(2), Rh1-P2-C20 105.9(2), C2-C1-C1'-C2' -84.3(8), C12-C11-C11'-C12' -37.7(11), C20-C19-C19'-C20' -92.6(8), C30-C29-C29'-C30' 40.2(10).



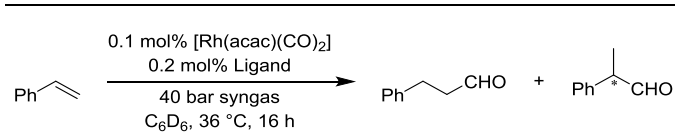
### Asymmetric hydrogenation (AH) of alkenes

Chiral monodentate phosphites,<sup>35</sup> phosphoramidites<sup>36</sup> and phosphonites<sup>8</sup> have proven to be effective ligands in the rhodium-catalysed AH of prochiral alkenes. We therefore tested the  $[\text{Rh}(\text{L}^{\text{P}})_2]\text{BF}_4$  complexes (*S*)-**10a** and (*R*)-**10b** against a selection of benchmark substrates, dimethyl itaconate (DMI) and the  $\alpha$ -acetamidoacrylates methyl 2-acetamidoacrylate (MAA) and methyl (*Z*)-2-acetamidocinnamate (MAC). In the AH of DMI we were able to obtain reasonable conversion after 48 h, however the reaction did not proceed enantioselectively. With the substrate MAA the conversion was low and with MAC it was negligible, however we did obtain a moderate *ee* for MAC when employing (*R*)-**10b** as ligand (see ESI for full details).

### Asymmetric hydroformylation (AHF) of styrene

The AHF of styrene analogues is an industrially relevant reaction due to the pharmacological importance of a number of the 2-aryl propionic acid derivatives accessible from the products of this reaction, for example (*S*)-naproxen, (*S*)-ibuprofen, (*R*)-flurbiprofen and (*S*)-ketoprofen are important non-steroidal anti-inflammatory drugs (NSAIDs).<sup>37</sup> However, the use of monodentate ligands in these transformations is underdeveloped. To the best of our knowledge, Beller and co-workers reported the best literature result for the AHF of styrene with a rhodium-phosphine complex (48% *ee*),<sup>38</sup> however the yield was poor, demonstrating the scope for progress in this area of research. Substitution of P–C bonds with P–O bonds in the ligand in hydroformylation catalysts often results in increased rates of reaction, as this facilitates the dissociation of CO from the metal.<sup>37</sup> Therefore we speculated that our MOP-phosphonite ligands could be promising candidates for this transformation due to their weak  $\sigma$ -donor but strong  $\pi$ -acceptor properties. We screened the six MOP-phosphonites and two MOP-phosphines in the AHF of styrene using 0.1 mol% of a catalyst prepared *in situ* from the reaction of  $[\text{Rh}(\text{acac})(\text{CO})_2]$  with the ligand in a Rh:P ratio of 1:2. The reactions were performed at a pressure of 40 bar syngas over 16h and at a moderate temperature of 36 °C (Table 4).

**Table 4** Rhodium-catalysed asymmetric hydroformylation of styrene.



	Ligand	Conversion <sup>a</sup>	<i>Iso/n</i> <sup>b</sup>	<i>ee</i> <sup>c</sup>
1	( <i>S</i> )-H-MOP	47	19	6 ( <i>S</i> )
2	( <i>R</i> )-MeO-MOP	53	24	6 ( <i>S</i> )
3	( <i>S</i> )- <b>1a</b>	99	18	3 ( <i>R</i> )
4	( <i>R</i> )- <b>1b</b>	>99	15	4 ( <i>S</i> )
5	( <i>S</i> )- <b>2a</b>	96	16	6 ( <i>R</i> )
6	( <i>R</i> )- <b>2b</b>	97	15	1 ( <i>R</i> )
7	( <i>S</i> )- <b>3a</b>	98	12	1 ( <i>S</i> )
8	( <i>R</i> )- <b>3b</b>	>99	16	12 ( <i>S</i> )

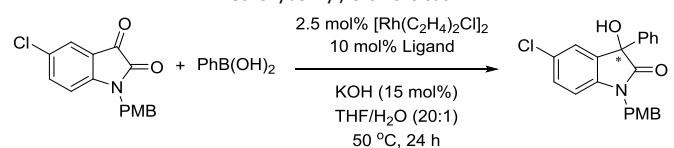
<sup>a</sup> % Conversion determined by <sup>1</sup>H NMR spectroscopy. <sup>b</sup> Ratio determined by <sup>1</sup>H NMR spectroscopy. <sup>c</sup> % *ee* determined by chiral GC (Supelco  $\beta$ -dex); absolute configuration was assigned according to literature data.

It is clear that the phosphonite ligands (Table 4, entries 3-8) far outperformed their phosphine counterparts (Table 4, entries 1 and 2) with respect to conversion. Very high conversions were obtained in each case, and complete conversion was achieved when the MeO-MOP phosphonites (*R*)-**1b** and (*R*)-**3b** were employed as the ligand. The product was a mixture of the linear (*n*) and branched (*iso*) isomers, however the desired *iso*-aldehyde was formed in a large excess; *iso/n* ratios ranged from 12-18 for the phosphonite catalysts (Table 4, entries 3-8) and was slightly higher (19-24) for the phosphine-catalysts (Table 4, entries 1 and 2). Unfortunately the enantioselectivity in these reactions was found to be low, the best result being a 12% *ee* when employing the ligand (*R*)-**3b** (Table 4, entry 8). However, the high conversions and regioselectivity observed in these non-optimised conditions with a low catalyst loading, does indicate that modified reaction conditions<sup>38</sup> and further ligand development could lead to promising AHF catalysts.

### Asymmetric addition of phenyl boronic acid to an isatin

Hayashi and co-workers reported the Rh-catalysed asymmetric addition of arylboronic acids to isatins in order to develop an asymmetric strategy towards the synthesis of biologically active compounds containing the 3-aryl-3-hydroxy-2-oxindole structural motif.<sup>39</sup> They were able to catalyse the reaction using a Rh(I)/(*R*)-MeO-MOP complex, achieving enantioselectivities of up to 91%. We therefore tested our series of MOP-phosphonite ligands in the addition of phenyl boronic acid to 1-(*p*-methoxybenzyl)-5-chloroisatin (Scheme 2). We also used the ligand (*R*)-MeO-MOP to allow us to compare our procedure to the literature data (ESI Table 2), both the conversion and *ee* are agreeable with the literature values.<sup>39</sup> Ligands (*S*)-**1a** and (*R*)-**1b** failed to provide any conversion, which we suspect is due to the reaction conditions that include water - both ligands are sensitive to hydrolysis.<sup>4c</sup> The biphenoxy derived ligands (*R*)-**2b**, (*S*)-**3a** and (*R*)-**3b** fared better however, generating conversions of between 40-43%. Ligand (*S*)-**2a** gave approximately half the conversion of (*R*)-**2b**, (*S*)-**3a** and (*R*)-**3b**, however we have found that this ligand is the most sensitive to decomposition out of the biphenoxy series, and this is possibly the reason for the reduced activity. The H-MOP-phosphonites (*S*)-**2a** and (*S*)-**3a** gave matching *ees* of 32%, however the MeO-MOP analogues gave very different *ees*. (*R*)-**3b** produced a low value of 11%, with (*R*)-**2b** giving the highest value of 39% *ee* in this biphenoxy series. We can also report, to the best of our knowledge, the first application of a Rh(I)/(*S*)-H-MOP complex as a catalyst in the asymmetric addition of phenylboronic acid to 1-(*p*-methoxybenzyl)-5-chloroisatin. The reaction gave complete conversion and achieved a good *ee* of 70% (see ESI Table 2 for full details of the conversions and enantioselectivities).

**Scheme 2** Rhodium-catalysed asymmetric addition of phenylboronic acid to 1-(*p*-methoxybenzyl)-5-chloroisatin.





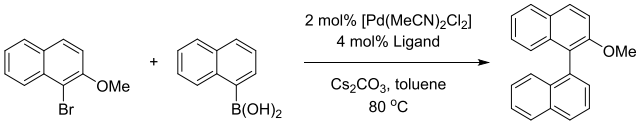
### Palladium(II) complexes and catalysis

One of the most frequently applied synthetic methodologies used to form carbon–carbon bonds is the palladium-catalysed Suzuki–Miyaura cross-coupling reaction of a boronic acid with an organic halide.<sup>40</sup> In these reactions, electron rich and bulky phosphine ligands are most often preferred,<sup>41</sup> however a DFT computational study by Harvey and co-workers into phosphine donor/acceptor properties and steric features found that the transmetallation process in the catalytic cycle has a lower energy barrier for weak  $\sigma$ -donor and strong  $\pi$ -acceptor ligands.<sup>42</sup> Iwasawa and co-workers have reported high yields and enantioselectivities (up to 91% and 78% respectively) in cross-coupling reactions of aryl chlorides employing bulky, chiral phosphonite ligands with low catalyst loadings (0.1 mol%).<sup>43</sup> We therefore synthesised palladium(II) dichloride complexes of our MOP-phosphonites and tested their ability to prepare axially chiral biaryl compounds from aryl bromides and aryl boronic acids, a field where a number of monophosphines have shown high enantioselectivities and activity.<sup>44</sup> The enantioselective synthesis of molecules with a binaphthyl backbone from naphthalene derivatives is interesting as this can facilitate a route to chiral monophosphine ligands such as those reported here. This was demonstrated by Ma and Yang who used a cross-coupling reaction as part of their strategy to obtain optically pure H-MOP.<sup>45</sup> It has also been reported that MeO-MOP stabilised palladium nanoparticles can catalyse the coupling of 1-bromo-2-methoxynaphthalene and naphthalene-1-boronic acid, albeit the unoptimised reaction gave only moderate conversion (50%) and low enantioselectivity (12%).<sup>46</sup> To the best of our knowledge there are no reports of MOP-phosphonite ligands being employed in this type of reaction.

#### Asymmetric Suzuki–Miyaura cross-coupling reactions

We tested our ligands in the palladium-catalysed reaction between 1-bromo-2-methoxynaphthalene and naphthalene-1-boronic acid in order to synthesise the axially chiral molecule 2-methoxy-1,1'-binaphthyl (Table 5). The catalyst was generated by stirring two equivalents of the corresponding ligand with  $[\text{Pd}(\text{MeCN})_2\text{Cl}_2]$  in DCM for 2 hours at room temperature, before removing the volatiles under vacuum; the catalysis was performed under the conditions stated. All of the MeO-MOP type ligands proceeded with almost full conversion. The reaction was complete within 30 minutes when (*R*)-**1b** was employed as the ligand and within 1 hour with (*R*)-MeO-MOP; longer reaction times were required to reach  $\geq 95\%$  conversions with (*R*)-**2b** and (*R*)-**3b**. The H-MOP ligands generally gave lower conversions and the reaction times were longer compared to their methoxy analogues. There was no additional conversion observed between 16 and 24 hours reaction times. The reactions with (*R*)-MeO-MOP and (*R*)-**1b** were the quickest in the series (Table 5, entries 2 and 4), however the enantioselectivity was negligible. It was markedly improved when using the biphenoxy based phosphonites (*R*)-**2b** and (*R*)-**3b**, which gave the highest enantioselectivities obtained (27% and 42% respectively). The diphenoxy derived phosphonite (*S*)-**1a** achieved the highest *ee* in the H-MOP ligand series, whereas (*R*)-**3b** was the best MeO-MOP ligand in this regard.

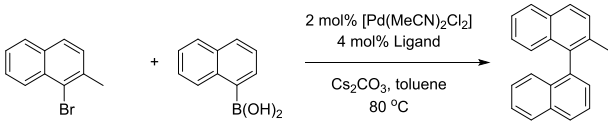
**Table 5** Asymmetric Suzuki–Miyaura coupling of naphthalene-1-boronic acid with 1-bromo-2-methoxynaphthalene.



	Ligand	Conversion <sup>a</sup>			<i>ee</i> <sup>b</sup>
		30 min	1 h	16 h	
1	( <i>S</i> )-H-MOP	86	94	95	4 ( <i>R</i> )
2	( <i>R</i> )-MeO-MOP	98	>99	–	8 ( <i>R</i> )
3	( <i>S</i> )- <b>1a</b>	66	83	94	21 ( <i>R</i> )
4	( <i>R</i> )- <b>1b</b>	>99	–	–	1 ( <i>S</i> )
5	( <i>S</i> )- <b>2a</b>	42	51	75	12 ( <i>R</i> )
6	( <i>R</i> )- <b>2b</b>	84	91	95	27 ( <i>R</i> )
7	( <i>S</i> )- <b>3a</b>	54	65	85	11 ( <i>S</i> )
8	( <i>R</i> )- <b>3b</b>	89	90	98	42 ( <i>R</i> )

<sup>a</sup> % Conversion determined by <sup>1</sup>H NMR spectroscopy. <sup>b</sup> % *ee* determined by chiral HPLC (Lux Cellulose) with hexane/2-propanol (99:1); absolute configuration was assigned according to literature data.

After screening the electron donating methoxy-substituted naphthalene, we were also interested in investigating the effects of replacing the methoxy functional group with a weakly donating methyl moiety. The result of the coupling reactions of 1-bromo-2-methylnaphthalene with naphthalene-1-boronic acid to synthesise 2-methyl-1,1'-binaphthyl are given in Table 6. In comparison to the results obtained with the methoxy substituted substrate, the conversions obtained are significantly lower in all cases and, with the exception of (*S*)-**1a** and (*S*)-**3a** (Table 6, entries 3 and 7), only a minor improvement to the conversion is made by leaving the reactions longer than 30 minutes. As with the methoxy substituted substrate, there was no additional conversion between 16 and 24 hours reaction times. The *ees* improved using 1-bromo-2-methylnaphthalene compared to 1-bromo-2-methoxynaphthalene - the value of the *ee* increased for every ligand used in our screening (Tables 5 and 6). There is no significant variation in the conversions observed between analogous ligands in the H-MOP and MeO-MOP series (Table 6), however there is a consistent pattern of the *ee* being higher for the MeO-MOP ligands in each case. The enantioselectivity for the diphenoxy ((*S*)-**1a**) and dimethylbiphenoxy ((*S*)-**3a**) phosphonites was similar (Table 6, entries 3 and 7), whereas it was noticeably lower for the biphenoxy ligand (*S*)-**2a**, which had an *ee* close to that obtained with the parent phosphine (*S*)-H-MOP (Table 6, entries 1 and 5). For the MeO-MOP series, the *ee* doubled upon changing the ligand from (*R*)-MeO-MOP to (*R*)-**1b**, however this was accompanied by a  $\sim 50\%$  reduction in the conversion (Table 6, entries 2 and 4). The ligands (*R*)-**2b** and (*R*)-**3b** achieved higher conversions than (*R*)-**1b**, with (*R*)-**2b** affording an *ee* similar to that of (*R*)-**1b**. However out of all the phosphines and phosphonites tested, (*R*)-**3b** achieved the highest *ee* of all (49%).

**Table 6** Asymmetric Suzuki-Miyaura coupling of naphthalene-1-boronic acid with 1-bromo-2-methylnaphthalene.


	Ligand	Conversion <sup>a</sup>			ee <sup>b</sup>
		30 min	1 h	16 h	
1	(S)-H-MOP	50	52	55	19 (S)
2	(R)-MeO-MOP	47	48	53	21 (S)
3	(S)- <b>1a</b>	26	31	38	30 (S)
4	(R)- <b>1b</b>	24	25	26	42 (S)
5	(S)- <b>2a</b>	32	33	40	17 (S)
6	(R)- <b>2b</b>	32	34	38	43 (S)
7	(S)- <b>3a</b>	27	38	46	32 (S)
8	(R)- <b>3b</b>	41	42	47	49 (S)

<sup>a</sup> % Conversion determined by <sup>1</sup>H NMR spectroscopy. <sup>b</sup> % ee determined by chiral HPLC (Lux Cellulose) with hexane/2-propanol (99:1); absolute configuration was assigned according to literature data.

### [Pd(L<sup>P</sup>)<sub>2</sub>Cl<sub>2</sub>] complexes

In an effort to investigate the solution and solid state properties of our Suzuki-Miyaura catalysts, we synthesised the complexes [Pd((S)-**3a**)<sub>2</sub>Cl<sub>2</sub>] (*S*)-**11a** and [Pd((R)-**3b**)<sub>2</sub>Cl<sub>2</sub>] (*R*)-**11b** by reacting [Pd(MeCN)<sub>2</sub>Cl<sub>2</sub>] with two equivalents of the corresponding phosphonite ligand in DCM. We were able to obtain single crystals of (*S*)-**11a** and (*R*)-**11b**, suitable for X-ray crystallographic analysis, from CDCl<sub>3</sub>/hexane and DCM/diethyl ether respectively. (*S*)-**11a** crystallised as two pseudo-polymorphs. One is in a monoclinic space group as a solvate with three chloroform molecules, whereas the second pseudo-polymorph is the same main molecule but in an orthorhombic space group with one chloroform molecule (ESI Figs. 8 and 9); an overlay image of the two pseudo-polymorphs has been provided (ESI Fig. 11). (*R*)-**11b** crystallised in a monoclinic space group and the asymmetric unit contains two disordered molecules of DCM in multiple orientations (Fig. 7). Both pseudo-polymorphs of (*S*)-**11a** and (*R*)-**11b** have a square-planar geometry about the palladium centre and the phosphonite ligands are in a *cis* orientation. The P–Pd–P bond angles are 99.79(5) and 101.16(3)° for (*S*)-**11a** and 100.73(4)° for (*R*)-**11b**. The Pd–P bond lengths range from 2.2234(9)–2.2331(15) Å in (*S*)-**11a** and 2.2354(11)–2.2329(11) Å in (*R*)-**11b** and the Pd–Cl bond lengths range from 2.3302(9)–2.3485(15) Å in (*S*)-**11a** and 2.3359(11)–2.3379(11) Å in (*R*)-**11b**. The X-ray structure of the complex [Pd((R)-MeO-MOP)<sub>2</sub>Cl<sub>2</sub>] was reported by Hayashi *et al.* and reveals that the MOP-phosphine ligands are in a *trans* orientation, unlike that seen for our MOP-phosphonite ligands; the Pd–P bond lengths in *trans*-[Pd((R)-MeO-MOP)<sub>2</sub>Cl<sub>2</sub>] are 2.339(2) and 2.344(15) Å and the P–Pd–P bond angle is 174.95(8)°. <sup>47</sup> The X-ray structure of a related complex with the chloride atoms replaced by fumaronitrile (*trans*-1,2-dicyanoethylene) and where the palladium is in a zero oxidation state, [Pd((S)-MeO-MOP)<sub>2</sub>(fumaronitrile)], was reported by Pregosin *et al.*; the molecule lies on a C<sub>2</sub> axis and the MOP-phosphine ligands are in a *cis* orientation, the P–Pd–P bond angle is 114.11(3)° and the Pd–P bond length is 2.3588(8) Å. <sup>48</sup>

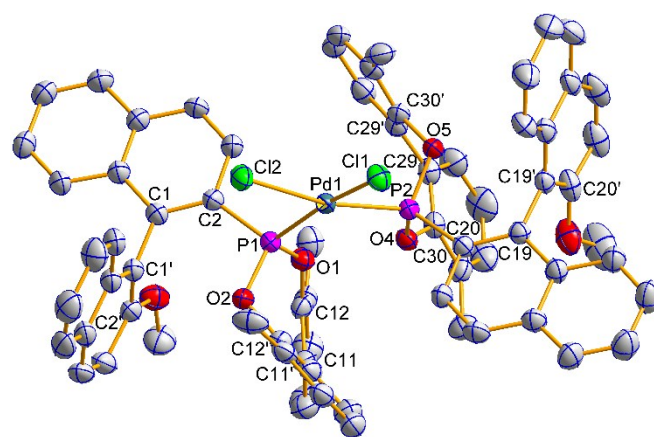


**Fig. 7** Molecular structure of (*R*)-**11b**. Hydrogen atoms have been omitted for clarity. Selected average bond distances (Å) and angles (°): Pd1–P1 2.2354(11), Pd1–P2 2.2329(11), Pd1–Cl1 2.3359(11), Pd1–Cl2 2.3379(11), P1–C2 1.793(4), P1–O1 1.605(3), P1–O2 1.593(3), P2–C20 1.806(4), P2–O4 1.586(3), P2–O5 1.595(3); P1–Pd1–P2 100.73(4), P1–Pd1–Cl1 169.34(4), P1–Pd1–Cl2 84.88(4), C2–C1–C1'–C2' –89.5(6), C12–C11–C11'–C12' 44.0(7), C20–C19–C19'–C20' –96.0(5), C30–C29–C29'–C30' 45.0(7).

The Pd–P bond lengths in these MeO-MOP-phosphine complexes are significantly longer than those found in our MOP-phosphonite complexes. A phosphonite complex analogous to (*S*)-**11a** and (*R*)-**11b**, *cis*-[Pd(P(OMe)<sub>2</sub>Ph)<sub>2</sub>Cl<sub>2</sub>], which has a crystallographic twofold rotation axis, has a Pd–P bond length of 2.2300(16) Å and a P–Pd–P bond angle of 100.88(2)°, values which are very similar to those found in (*S*)-**11a** and (*R*)-**11b**. <sup>49</sup> We analysed (*S*)-**11a** and (*R*)-**11b** in solution by multinuclear NMR spectroscopy. For (*S*)-**11a** we observed two broad peaks in the <sup>31</sup>P{<sup>1</sup>H} NMR spectrum at 25 °C, a large peak at 144.3 ppm and a smaller peak at 142.8 ppm, which correspond to the *cis* and *trans* isomers. In the case of (*R*)-**11b** one broad peak was observed at approximately 140 ppm in the <sup>31</sup>P{<sup>1</sup>H} NMR spectrum at room temperature.

### Conclusions

We have used experimental and computational data to quantify the stereoelectronic donor properties within a MOP-phosphonite ligand series, and rationalised previously reported findings that rotation about the aryl–aryl junction in the biphenyl moiety of (*S*)-**2a**, (*R*)-**2b**, (*S*)-**3a** and (*R*)-**3b** is unrestricted under standard conditions. We prepared Rh(I) complexes and through detailed NMR and X-ray crystallographic analyses of them, have proven the existence of M–π interactions in complexes of the type [Rh(L<sup>P</sup>)<sub>2</sub>]<sup>+</sup>, with one ligand acting as a chelating P,C-π-donor. In the rhodium-catalysed AHF reaction of styrene, our ligands proved to be high yielding and regioselective for the branched isomer with low catalyst loadings. Palladium dichloride complexes of the MOP phosphonite ligands were synthesised and characterised in detail, and they were then shown to be effective as catalysts in asymmetric Suzuki-Miyaura cross-coupling reactions, with full conversions and enantioselectivities of up to 49% possible, depending on the substrates investigated.

## Acknowledgements

We acknowledge the financial support of the EPSRC for a Fellowship award (LJH: EP/G005206/1) and their National Mass Spectrometry Facility at Swansea. We also thank the School of Chemistry, Newcastle University for a Studentship (JTF).

## Notes and references

- (a) *Phosphorus Ligands in Asymmetric Catalysis*, ed. A. Börner, Wiley-VCH, Weinheim, 2008; (b) *Phosphorus(III) Ligands in Homogeneous Catalysis: Design and Synthesis*, ed. P. C. J. Kamer and P. W. N. M. van Leeuwen, John Wiley & Sons, Chichester, 2012.
- F. Lagasse and H. B. Kagan, *Chem. Pharm. Bull.*, 2000, **48**, 315.
- A. Ficks, W. Clegg, R. W. Harrington and L. J. Higham, *Organometallics*, 2014, **33**, 6319.
- (a) A. Ficks, R. M. Hiney, R. W. Harrington, D. G. Gilheany and L. J. Higham, *Dalton Trans.*, 2012, **41**, 3515; (b) A. Ficks, R. W. Harrington and L. J. Higham, *Dalton Trans.*, 2013, **42**, 6302; (c) J. T. Fleming, A. Ficks, P. G. Waddell, R. W. Harrington and L. J. Higham, *Dalton Trans.*, 2016, **45**, 1886.
- L. Bini, C. Muller and D. Vogt, *Chem. Commun.*, 2010, **46**, 8325.
- R. Bayersdörfer, B. Ganter, U. Englert, W. Keim and D. Vogt, *J. Organomet. Chem.*, 1998, **552**, 187.
- Jarl I. van der Vlugt, Jos M. J. Paulusse, Eric J. Zipp, Jason A. Tijmensen, Allison M. Mills, Anthony L. Spek, C. Claver and D. Vogt, *Eur. J. Inorg. Chem.*, 2004, 4193.
- (a) C. Claver, E. Fernandez, A. Gillon, K. Heslop, D. J. Hyett, A. Martorell, A. G. Orpen and P. G. Pringle, *Chem. Commun.*, 2000, 961; (b) M. T. Reetz and T. Sell, *Tetrahedron Lett.*, 2000, **41**, 6333; (c) Y. Fu, G.-H. Hou, J.-H. Xie, L. Xing, L.-X. Wang and Q.-L. Zhou, *J. Org. Chem.*, 2004, **69**, 8157.
- (a) W. McFarlane and D. S. Rycroft, *J. Chem. Soc., Chem. Commun.*, 1972, 902; (b) W. McFarlane and D. S. Rycroft, *J. Chem. Soc., Dalton Trans.*, 1973, 2162.
- (a) R. P. Pinnell, C. A. Megerle, S. L. Manatt and P. A. Kroon, *J. Am. Chem. Soc.*, 1973, **95**, 977; (b) D. W. Allen and B. F. Taylor, *J. Chem. Soc., Dalton Trans.*, 1982, 51.
- (a) S. Vastag, B. Heil and L. Markó, *J. Mol. Catal.*, 1979, **5**, 189; (b) A. Roodt, S. Otto and G. Steyl, *Coord. Chem. Rev.*, 2003, **245**, 121.
- R. A. Baber, M. F. Haddow, A. J. Middleton, A. G. Orpen, P. G. Pringle, A. Haynes, G. L. Williams and R. Papp, *Organometallics*, 2007, **26**, 713.
- C. A. Tolman, *Chem. Rev.*, 1977, **77**, 313.
- M. Carreira, M. Charernsuk, M. Eberhard, N. Fey, R. van Ginkel, A. Hamilton, W. P. Mul, A. G. Orpen, H. Phetmung and P. G. Pringle, *J. Am. Chem. Soc.*, 2009, **131**, 3078.
- (a) A. Pidcock, R. E. Richards and L. M. Venzani, *J. Chem. Soc. A*, 1966, 1707; (b) S. O. Grim, R. L. Keiter and W. McFarlane, *Inorg. Chem.*, 1967, **6**, 1133.
- K. B. Dillon, A. E. Goeta, P. K. Monks and H. J. Shepherd, *Polyhedron*, 2010, **29**, 606.
- K. M. Anderson and A. G. Orpen, *Chem. Commun.*, 2001, 2682.
- M. J. Atherton, J. Fawcett, A. P. Hill, J. H. Holloway, E. G. Hope, D. R. Russell, G. C. Saunders and R. M. J. Stead, *J. Chem. Soc., Dalton Trans.*, 1997, 1137.
- (a) A. D. Becke, *J. Chem. Phys.*, 1993, **98**, 5648; (b) P. J. Stephens, F. J. Devlin, C. F. Chabalowski and M. J. Frisch, *J. Phys. Chem.*, 1994, **98**, 11623.
- (a) H. M. Senn, D. V. Deubel, P. E. Blöchl, A. Togni and G. Frenking, *J. Mol. Struct. Theochem*, 2000, **506**, 233; (b) C. H. Suresh and N. Koga, *Inorg. Chem.*, 2002, **41**, 1573; (c) N. Fey, A. G. Orpen and J. N. Harvey, *Coord. Chem. Rev.*, 2009, **253**, 704.
- T. L. Brown and K. J. Lee, *Coord. Chem. Rev.*, 1993, **128**, 89.
- B. J. Dunne, R. B. Morris and A. G. Orpen, *J. Chem. Soc., Dalton Trans.*, 1991, 653.
- K. D. Cooney, T. R. Cundari, N. W. Hoffman, K. A. Pittard, M. D. Temple and Y. Zhao, *J. Am. Chem. Soc.*, 2003, **125**, 4318.
- J. Mathew, T. Thomas and C. H. Suresh, *Inorg. Chem.*, 2007, **46**, 10800.
- (a) A. Almenningen, O. Bastiansen, L. Fernholt, B. N. Cyvin, S. J. Cyvin and S. Samdal, *J. Mol. Struct.*, 1985, **128**, 59; (b) S. Charbonnier, S. T. Beguems, Y. T. N'Guessan, D. Legoff, A. Proutiere and R. Viani, *J. Mol. Struct.*, 1987, **158**, 109; (c) F. Grein, *J. Phys. Chem. A*, 2002, **106**, 3823; (d) E. Masson, *Org. Biomol. Chem.*, 2013, **11**, 2859.
- E. L. Eliel and S. H. Wilen, *Stereochemistry of Organic Compounds*, John Wiley & Sons, New York, 1994.
- R. Shintani, C. Takagi, T. Ito, M. Naito and K. Nozaki, *Angew. Chem., Int. Ed.*, 2015, **54**, 1616.
- R. Shintani, H. Kurata and K. Nozaki, *Chem. Commun.*, 2015, **51**, 11378.
- (a) M. Sakai, M. Ueda and N. Miyaoura, *Angew. Chem., Int. Ed.*, 1998, **37**, 3279; (b) E. F. Clarke, E. Rafter, H. Müller-Bunz, L. J. Higham and D. G. Gilheany, *J. Organomet. Chem.*, 2011, **696**, 3608.
- X. Shen and S. L. Buchwald, *Angew. Chem., Int. Ed.*, 2010, **49**, 564.
- H. Bircher, B. R. Bender and W. von Philipsborn, *Magn. Reson. Chem.*, 1993, **31**, 293.
- J. D. Heise, D. Raftery, B. K. Breedlove, J. Washington and C. P. Kubiak, *Organometallics*, 1998, **17**, 4461.
- D. Selent, W. Baumann, R. Kempe, A. Spannenberg, D. Röttger, K.-D. Wiese and A. Börner, *Organometallics*, 2003, **22**, 4265.
- A. R. O'Connor, W. Kaminsky, D. M. Heinekey and K. I. Goldberg, *Organometallics*, 2011, **30**, 2105.
- M. T. Reetz and G. Mehler, *Angew. Chem., Int. Ed.*, 2000, **39**, 3889.
- (a) M. van den Berg, A. J. Minnaard, E. P. Schudde, J. van Esch, A. H. M. de Vries, J. G. de Vries and B. L. Feringa, *J. Am. Chem. Soc.*, 2000, **122**, 11539; (b) Y. Fu, X.-X. Guo, S.-F. Zhu, A.-G. Hu, J.-H. Xie and Q.-L. Zhou, *J. Org. Chem.*, 2004, **69**, 4648.
- R. Franke, D. Selent and A. Börner, *Chem. Rev.*, 2012, **112**, 5675.
- G. Erre, S. Enthaler, K. Junge, S. Gladiali and M. Beller, *J. Mol. Catal. A: Chem.*, 2008, **280**, 148.
- R. Shintani, M. Inoue and T. Hayashi, *Angew. Chem., Int. Ed.*, 2006, **45**, 3353.
- N. Miyaoura and A. Suzuki, *Chem. Rev.*, 1995, **95**, 2457.
- (a) U. Christmann and R. Vilar, *Angew. Chem., Int. Ed.*, 2005, **44**, 366; (b) R. Martin and S. L. Buchwald, *Acc. Chem. Res.*, 2008, **41**, 1461.
- J. Jover, N. Fey, M. Purdie, G. C. Lloyd-Jones and J. N. Harvey, *J. Mol. Catal. A: Chem.*, 2010, **324**, 39.
- T. Kamei, A. H. Sato and T. Iwasawa, *Tetrahedron Lett.*, 2011, **52**, 2638.
- D. Zhang and Q. Wang, *Coord. Chem. Rev.*, 2015, **286**, 1.
- Y.-N. Ma and S.-D. Yang, *Chem. Eur. J.*, 2015, **21**, 6673.
- K. Sawai, R. Tatumi, T. Nakahodo and H. Fujihara, *Angew. Chem., Int. Ed.*, 2008, **47**, 6917.
- Y. Uozumi, K. Kitayama, T. Hayashi, K. Yanagi and E. Fukuyo, *Bull. Chem. Soc. Jpn.*, 1995, **68**, 713.
- P. Dotta, P. G. A. Kumar, P. S. Pregosin and A. Albinati, *Helv. Chim. Acta*, 2004, **87**, 272.
- A. M. Z. Slawin, P. G. Waddell and J. D. Woollins, *Acta Cryst. E*, 2010, **66**, m321.

